

BEHAVIOR OF SnO₂ IN THE TIN-BEARING IRON CONCENTRATE DURING A REDUCTION SINTERING PROCESS

Z. Su, Y. Zhang*, B. Liu, J. Chen, G. Li, T. Jiang**

Central South University, School of Minerals Processing and Bioengineering, Changsha, China

(Received 31 October 2015; accepted 14 December 2016)

Abstract

The reserve of tin-bearing iron ores is very large in China. However, they have not been utilized sufficiently so far due to the complex embedded relationship between iron- and tin-bearing minerals. In the present work, the behavior of tin in the tin-bearing iron concentrates during a reduction sintering process (RSP) were studied using XRD, SEM-EDS, chemical valence state analysis and morphology analysis. The results show that there is about 30 mass% tin deprived from the tin-bearing iron concentrates by the RSP. The tin-bearing phases remained in the finished sinters exist as the form of stannic (Sn⁴⁺), stannous (Sn²⁺) compounds and metallic Sn (Sn⁰). The atmosphere in the sinter bed during the RSP is theoretically suitable for the volatilization of SnO_(g). However, the gas composition and temperature of the sintering gas flow are changeable, which bring about adverse effect to the deprivation of tin.

Keywords: Reduction sintering; Tin-bearing iron concentrate; Tin removal; SnO₂

1. Introduction

Tin-bearing iron ore is recognized as one of typically complex iron ore resources in China, of which the reserve is more than 0.5 billion tons [1]. Present physical mineral processing methods are difficult to separate tin from iron oxides because cassiterite is closely embedded and fine-grained dissemination in the iron ores [2-4]. The tin content remained in the final iron concentrates after multistage beneficiation is still in excess of 0.08 mass%. Steel production practice has proved that tin in the raw materials is difficult to remove during the subsequent ironmaking and steelmaking processes, and it will reduce the mechanical performances of steel products. Therefore, these tin-bearing iron concentrates can't be used as ironmaking burdens directly [5, 6].

Great efforts have been made to utilize the tin-bearing iron concentrates and the reduction behavior of SnO₂ under CO-CO₂ atmosphere has been investigated by the authors' group [5-11]. For instance, selective sulfurization and chlorination roasting processes are effective to separate tin from the concentrates, but the environmental pollution and equipment corrosion is unavoidable [5, 12, 13]. Another selective reduction volatilization (SRV) process of tin recovery and pellet preparation for blast furnace iron-making from the tin-bearing iron

concentrates, namely a coal-based rotary kiln direct reduction (DR) process, has been developed and successfully performed in the pilot-scale and semi-industrialization tests by the authors' group [11, 14]. However, grate-kiln DR process has a low productivity to utilize the huge reserve of tin-bearing iron ores. In addition, with continuous exhaustion of iron ore resources, high-quality iron ores become increasingly scarce in China. Therefore, to utilize these tin-bearing iron concentrate is very important to save iron and tin resources.

It is known that iron ore sintering is one of the most important processes in the steel manufacturing industry. Over the years, a number of innovative techniques have been developed to boost the efficiency of the sintering process and reduce the environmental pollution. It was reported that using pre-reduced agglomerate (PRA) process to prepare BF burdens could reduce more than 10% of CO₂ emissions in total of the ironmaking process [15]. And another process of pellets-metallized sintering process (PMSP) is effective to treat the zinc-bearing dusts from iron and steel companies, and more than 90% of Zn can be removed from the dusts [16]. It was also found that part of tin could be removed from tin-bearing iron concentrates by a reduction sintering process (RSP) [2]. As reported, the residual tin content in the finished sinters was less than 0.08 mass% under optimal conditions for RSP, and the

Corresponding authors: zybcsu@126.com*, jiangtao@csu.edu.cn**



finished sinters could be used as qualified BF burdens. Tin-rich dusts could be recovered from the dedusting system. It seems that the RSP should be an effective way to utilize the tin-bearing iron concentrates based on the existing sintering machines. Nevertheless, there is no further research on the RSP and the RSP is still not put into practice. Thus the behavior of SnO_2 during the RSP needs to be investigated further.

In order to confirm the deprivation efficiency of Sn from the tin-bearing iron concentrates by the RSP and determining the existence form of Sn in the finished sinters, sinter pot tests were conducted using the tin-bearing iron concentrates as raw materials. In addition, the behavior of SnO_2 in the tin-bearing iron concentrates during the RSP was investigated using chemical valence state analysis, XRD, SEM-EDS and optical microscopy.

2. Materials and method

2.1. Materials

2.1.1. Tin-bearing iron concentrates

The tin-bearing iron concentrates used in this study were taken from the Inner Mongolia Autonomous Region, China. The mass percentage of the samples with granularity below 0.075 mm was found as 81.4 mass%. The main chemical compositions given in Table 1 were determined by X-ray fluorescence (XRF, Axios mAX, Holand PANalytical Co., Ltd). The X-ray diffraction pattern (XRD, D/max 2550PC, Japan Rigaku Co., Ltd) of the sample is presented in Fig. 1.

It can be seen from Table 1 that the total iron content (TFe) of the sample was 64.480 mass%, and the content of tin, 0.230 mass%, exceeded the limitation of the iron-making materials ($\text{Sn} < 0.08$ mass%). As shown in Fig. 1, the major mineral phase in the concentrate is magnetite as well as a small amount of quartz. Our former study on the mineralogy of a similar sample from the same mine demonstrated that the main tin-bearing mineral in the iron concentrates was cassiterite, which was closely embedded in the magnetite particles [4-6]. A chemical analytic method to determine calcium carbonate was used to measure the actual content of CaCO_3 in the

Table 1. Chemical composition of the sample concentrates

Components	TFe	FeO ^a	SiO ₂	Al ₂ O ₃	CaO	MgO	Sn	S
Mass fraction (mass%)	64.480	24.65	4.402	0.870	2.492	0.691	0.230	0.070

^a FeO content is analyzed by a chemical method.

Table 2. Proximate analysis of coke breeze (on dry basis) and chemical composition of its ash (mass fraction, mass%)

Proximate analysis			Chemical composition of the ash					S _{total}
Ash	Volatile	Fixed Carbon	TFe	SiO ₂	CaO	Al ₂ O ₃	MgO	
15.56	1.86	82.58	1.77	7.11	0.35	1.82	0.08	0.07

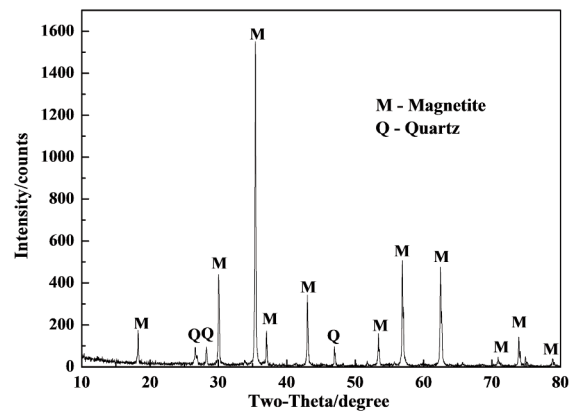


Figure 1. XRD pattern of the tin-bearing iron concentrates

concentrates. It was observed that 66.1 mass% of the calcium existed in the form of calcium carbonate, which was similar to the previous result [4].

2.1.2. Lime

The lime powder, used for adjusting the basicity of the sinter mixture, was firstly ground to a particle size passing through a 0.074 mm sieve. The CaO content of lime is tested as 75.10 mass% by a chemical analytic method.

2.1.3. Coke breeze

Proximate analysis of coke breeze used as solid fuel is given in Table 2. The coke breeze was in advance ground below 0.5 mm and then sieved into three kinds of particle size of -0.075 mm, 0.075-0.150 mm and 0.150-0.5 mm.

2.1.4. Gases

The purity of gases (CO , CO_2 and N_2) used was higher than 99.99 vol.%.

2.2. Methods

Both the conventional sintering process and RSP tests were conducted in a laboratorial sinter pot. The schematic diagram of the sinter pot is shown in Fig. 2.

Based on the foregoing research [2, 15, 16], the detailed procedure of RSP was given as follows: To begin with, the tin-bearing iron concentrates, fine coke



powder and lime were proportioned and mixed manually, and the mixture was balled into 3-8 mm diameter green pellets in a $\Phi 1000$ mm disc pelletizer. Then, the pellets were charged into the sinter pot. Before charging the pellets, refractory bricks with particle size of 3-10 mm were placed into the sinter pot to protect the pot grates. Ignition was conducted at 1150 °C for 1.5 min under suction pressure of 5 kPa, and natural gas was used as ignition fuel. After ignition, sintering was performed at an initial suction pressure of 10 kPa. Subsequently, the sintered cake was cooled for 3 min at 5 kPa suction pressure. During the sintering process, the flue gas components of outlet and the sinter bed were analyzed by using a flue gas analyzer (MRU-VARIO PLUS, Germany) from sampling point A (in the vacuum chamber for testing the outlet flue gases compositions) and B (20 cm below the mixture surface for testing the flue gas components and temperature in the sinter bed) as presented in Fig. 2. In addition, temperature in the sinter bed is measured by a thermocouple Type S (PtRh-Rh) in sampling point A and B [17, 18]. Finally, the cooled sinter cake was discharged, crushed and sampled in three areas as shown in Fig. 2.

The sampled sinters were first divided into two parts. One part was finely ground to 100% less than 0.074 mm for chemical valence state analysis and XRD analysis. Chemical valence state analysis of Fe includes the content of Fe^{3+} , Fe^{2+} and Fe^0 [19-21]. The contents of Sn^{4+} , Sn^{2+} and Sn^0 were also analyzed by means of chemical valence state method [8, 22, 23].

The other part of the sampled sinter was prepared for morphology analysis. Optical microscopy (LEICA, DMI5000 M, Germany) was used to observe the microstructure. The elemental composition of the main mineral in the sample was analyzed using environmental scanning electron microscopy (ESEM);

FEI QUANTA 200; FEI, Eindhoven, The Netherlands) equipped with an EDAX energy dispersive X-ray spectroscopy (EDS) detector (EDAX Inc., Mahwah, NJ).

2.3. Evaluation Indexes

The volatilization ratio of tin in each test was calculated as follow:

$$\gamma = \left(1 - \frac{m1 \cdot \alpha}{m1 \cdot \beta}\right) \times 100$$

where γ is the volatilization ratio of tin (mass%), α is the tin mass contents in the sinter (mass%), β is the tin mass contents in the raw mixture (in dry basis) (mass%), $m1$ is the mass of the raw mixture (in dry basis) (g), $m2$ is the mass of the sinter after the sintering process (g).

3. Results and discussion

3.1. Effect of primary parameters on the removal of Sn

Based on the previous research [2], sinter pot tests were conducted to study the effects of the main parameters, including coke particle size, coke dosage and basicity ($R = \text{CaO}/\text{SiO}_2$ ratio), on the residual tin content of the finished sinters. The final results are displayed in Table 3. Fig. 3 shows the effect of coke dosage on the residual tin content of the sinters and the tin volatilization ratio.

As shown in Fig. 3 and Table 3, the coke dosage has a more obvious impact on the removal of tin compared to coke particle size and basicity. The residual tin content of the sinters decreases from 0.221 mass% down to 0.171 mass% and the tin volatilization fraction increases from 2.3 mass% up to

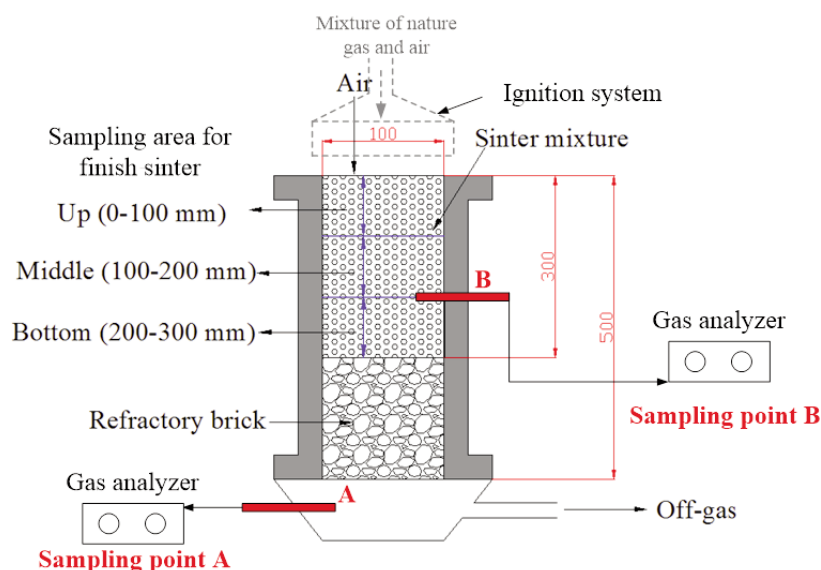


Figure 2. Schematic diagram of the sinter pot

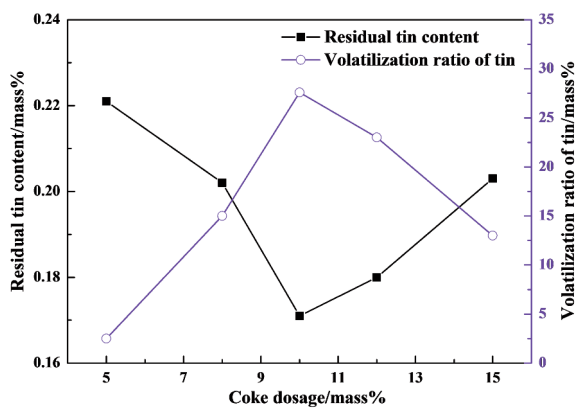
Table 3. Effect of primary sintering parameters on the residual tin content in the sinters

Test No.	Coke dosage	Coke size	Basicity	Residual tin content (mass %)	
	(mass %)	(mm)	($R=CaO/SiO_2$)	Stratified samples	Average
1	5.0	0.075-0.150 (100 mass %)	Natural basicity 0.6	-	0.221
2	8.0			-	0.202
3	12.0			-	0.180
4	15.0			-	0.203
5	10.0	0.075-0.150 (100 mass %)	Natural basicity 0.6	Upper: 0.213	0.171
				Middle: 0.172	
				Bottom: 0.156	
6		0.150-0.5 (100 mass %)		-	0.206
7		-0.075 (100 mass %)		-	0.193
8	10.0	0.075~0.150 (100 mass %)	1.0	-	0.18
9			2.0	-	0.192

29.6 mass% when the coke dosage increases from 5.0 mass% to 10.0 mass%. However, the tin volatilization ratio decreases when the coke dosage exceeds 10.0 mass%. Coke dosage of 10.0 mass% is recommended as the favorable value.

It is also listed in Table 3 (Test No. 5-9) that the basicity has a slight impact on the residual tin content in the sinters. An increase of the basicity counts against removing tin from the sinters. Fine-grained or coarse-grained coke breeze also has an adverse effect on the removal of tin.

It is noteworthy that the residual tin content of three stratified samples (Test No. 5 in Table 3) has a remarkable difference. The value decreases from 0.213 mass% to 0.156 mass% at the sampling point varying from the upper to the bottom. It seems that the sintering conditions in the bottom layer are helpful to the removal of tin.

**Figure 3.** Effect of coke dosage on the residual tin content and the tin volatilization ratio

In order to further investigate the effect of tin content in the sinter mixture on the tin volatilization ratio and the residual tin content in the sinters, the tin-bearing iron concentrates were blended with an ordinary magnetite concentrates (containing 65.423 mass% of Fe and 0.001 mass% of Sn) as mass ratio of 2:1 and 1:1 (Test No. 10-11), that is to say, the tin content in the sinter mixture is 0.183 mass% and 0.115 mass%, respectively. Then, the sinter pot tests were conducted as the same method described in Section 2.2 under the optimal sintering conditions: coke dosage of 10.0 mass%, coke particle size of 0.075-0.150 mm and natural basicity. The results presented in Table 4 indicated that the volatilization ratio of tin were almost about 30 mass% and the residual tin content in the finished sinters could be decreased to 0.079 mass% as the tin content in the sinter mixture was 0.115 mass% (Test No. 11). Therefore, it is concluded that the tin content of the sinter mixture should be controlled below 0.12 mass% in order to produce qualified sinters (tin content required to be less than 0.08 mass%) for BF ironmaking by the RSP.

Table 4. Effect of tin content of sinter mixture on the tin volatilization ratio and the residual tin content

Test No.	Tin content in the sinter mixture (mass%)	Residual tin content in the finished sinters (mass%)	Tin volatilization ratio
			(mass%)
5	0.230	0.171	26.6
10	0.183	0.140	30.5
11	0.115	0.079	32.2

3.2. Phase compositions of the finished sinters

Phase compositions of the sinters produced at different coke dosage (Test No. 1 and No. 5 in Table 3) were examined by XRD and the results are presented in Fig. 4. The XRD pattern of sample 1[#] indicates that the major mineral constituents of the sinters are hematite (Fe₂O₃) and magnetite (Fe₃O₄). Part of magnetite is oxidized into hematite due to the oxidation atmosphere in the sinter layer. It is inferred from the XRD pattern of sample 5[#] that part of magnetite (Fe₃O₄) is reduced to wustite (FeO) at the coke dosage of 10.0 mass%. However, trace amount of tin-bearing phases in the finished sinters can't be determined by XRD. Thus, it will be examined in another way.

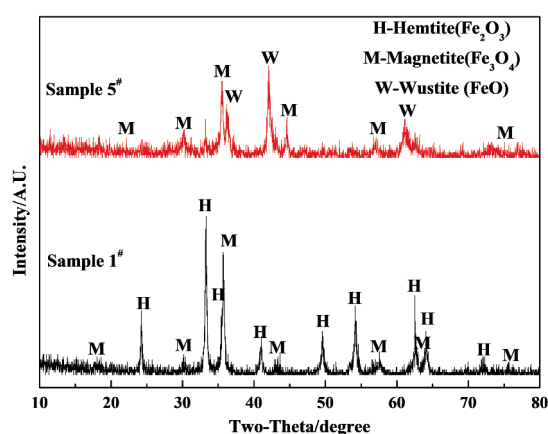


Figure 4. XRD patterns of the sinters with different coke dosage (Sample 1[#]: coke dosage of 5.0 mass%; Sample 5[#]: coke dosage of 10.0 mass%)

3.3. Chemical valence state analysis of Sn and Fe in the sinters

As observed in Table 3, the residual tin content in the sinters has a noteworthy difference under the condition of 5.0 mass% and 10.0 mass% coke dosage (Test No.1 and No. 5). For comparison, chemical valence state analysis results of Fe and Sn in the sinter samples (Sample 1[#] and Sample 5[#]) and the raw tin-bearing iron concentrates are demonstrated in Table 5.

The results presented in Table 5-(a) and (b) reveal that most of FeO (Fe²⁺) in the raw concentrates is easily oxidized to Fe₂O₃ (Fe³⁺) when the coke dosage is 5.0 mass%. And the content of SnO₂ (Sn⁴⁺) almost keeps unchanged, which further indicates that the tin oxide is very difficult to be removed when the coke dosage is low. It is observed from Table 5-(c) that the distribution ratio of FeO (Fe²⁺) in total Fe is 66.5%, and a small amount of iron oxides is reduced to metallic iron (Fe⁰) in the sample 5[#]. Meanwhile, the distribution ratio of stannous (Sn²⁺) compound and

metallic tin (Sn⁰) in the total Sn is 28.1% and 49.7%, respectively. The results are in accordance with the thermodynamics calculation that Fe₂O₃ and SnO₂ can be reduced stepwise according to Fe₂O₃→Fe₃O₄→FeO→Fe and SnO₂→SnO→Sn [13, 14].

Furthermore, it is observed from Table 5-(b) and (c) that most residual tin exists in the form of stannic(Sn⁴⁺) and stannous(Sn²⁺) compounds in the finished sinters. The possible phase transformation of SnO₂ during the RSP would be further discussed in the future study.

Table 5. Chemical valence state analyses of Fe and Sn in the iron concentrate and sinter (mass %)

(a) Tin-bearing iron concentrate				
Chemical valence state	Fe ³⁺	Fe ²⁺	Fe ⁰	Total
Content	45.3	19.2	0	64.5
Distribution in total Fe	70.2	29.8	0	100
Chemical valence state	Sn ⁴⁺	Sn ²⁺	Sn ⁰	Total
Content	0.230	0	0	0.230
Distribution in total Sn	100	0	0	100
(b) Sample 1 [#] (5.0 mass% coke dosage)				
Chemical valence state	Fe ³⁺	Fe ²⁺	Fe ⁰	Total
Content	54.8	8.3	0	62.1
Distribution in total Fe	86.6	13.4	0	100
Chemical valence state	Sn ⁴⁺	Sn ²⁺	Sn ⁰	Total
Content	0.202	0.015	0	0.217
Distribution in total Sn	93.1	6.9	0	100
(c) Sample 5 [#] (10.0 mass% coke dosage)				
Chemical valence state	Fe ³⁺	Fe ²⁺	Fe ⁰	Total
Content	21.6	45.3	1.2	68.1
Distribution in total Fe	31.7	66.5	1.8	100
Chemical valence state	Sn ⁴⁺	Sn ²⁺	Sn ⁰	Total
Content	0.038	0.048	0.085	0.171
Distribution in total Sn	22.2	28.1	49.7	100

3.4. Morphology analysis

Morphology analysis was conducted to confirm the microstructure feature of the sinters (Sample 5[#]) by means of an optical microscope and scanning electron microscopy. The result is presented in Fig. 5.

It can be seen from Fig. 5-(a) and (b) that most iron oxides exist in wustite (FeO) with a typically rounded structure, and a small amount of metallic iron with a bright-white color is also observed. The mineral phase (Spot A in Fig. 5-(c)) is Fe-Sn alloy confirmed by EDS analysis in Fig. 5-(d). And Fe-Sn alloy is closely connected with wustite particles (Spot

B in Fig. 5-(c)).

The results indicate that a few of tin and iron oxides are synchronously reduced to the metallic state under the partial reductive atmosphere in the sinter bed. Fe-Sn alloy is easily formed when metallic Sn coexists with metallic Fe, which has obviously negative influence on the removal of tin. The results agree with the findings reported in the previous research [5, 6].

3.5. Emission rules of the flue gas during the RSP

The emission rules of O₂, CO, CO₂, CO/(CO+CO₂) content and temperature of the outlet flue gas with different coke dosage (Test No. 1 and No. 4 in Table 3) are presented in Fig. 6.

Fig. 6-(a) shows the emission rules of outlet flue gas with 5.0 mass% of coke. The O₂ content of the off-gas decreases obviously from 21.0 vol.% to 9.0 vol.% during the ignition stage and then it gradually increased and maintained at 10.0 vol.%. After the ignition stage, the CO, CO₂ and CO/(CO+CO₂) content of the outlet flue gas was stabilized at 1.5-2.0 vol.%, 10.0-11.0 vol.% and 14.5-15.0 %, respectively. Approaching to the end of sintering, CO, CO₂ and CO/(CO+CO₂) content decreased to nearly zero while O₂ content increased rapidly to 21.0 vol.%. The temperature of the outlet flue gas was almost unchanged at 50-60 °C during the in the initial period of the sintering process, and then it increased rapidly to the top and decreased again. The sintering end point was determined based on the top sintering temperature of the outlet flue gas. The sintering time increased obviously when the coke dosage increased

to 15.0 mass%. The emission rules of the outlet flue gas presented in Fig. 6-(b) was similar to that of Fig. 6-(a) when the coke dosage increased to 15.0 mass%. In addition, the value of O₂, CO, CO₂ and CO/(CO+CO₂) content maintained during the RSP was 6.0-7.0 vol.%, 5.0-5.5 vol.%, 11.0-11.5 vol.% and 34.0-35.0 %.

The changing rules of O₂, CO, CO₂ content of the flue gas and temperature in the sinter bed at coke dosage of 5.0 mass% were shown in Fig. 7.

The results in Fig. 7 indicated that the changing rules of the gas components were nearly consistent with the results of the outlet flue gas as shown in Fig. 6-(a). The consumption of O₂ was due to the combustion of coke during the sintering process. Coke breeze started to combust when the temperature of sinter bed was higher than 1000 °C and the temperature increased sharply to 1350 °C, while the high-temperature residence time of higher than 1000 °C was only about 5.0 min. Approaching the end of sintering, O₂ content increased rapidly to 21 vol.%.

Compared with the results of Fig. 6 and Fig. 7, it can be concluded that the flue gas components in the sinter bed are similar to those of the outlet flue gas. And the flue gas components in the sinter bed can be regarded as the flue gas from the upper layer. The CO/(CO+CO₂) value of the flue gas was about 15.0-35.0 % when the coke dosage increased from 5.0 mass% to 15.0 mass%, and the total sintering time increased with the increase of coke dosage as well. In addition, the high-temperature residence time (> 1000 °C) also increases as the coke dosage, but it was still not enough for removing tin from the sinters. The results were summarized in Table 6, the sintering process was divided into two stages based on the

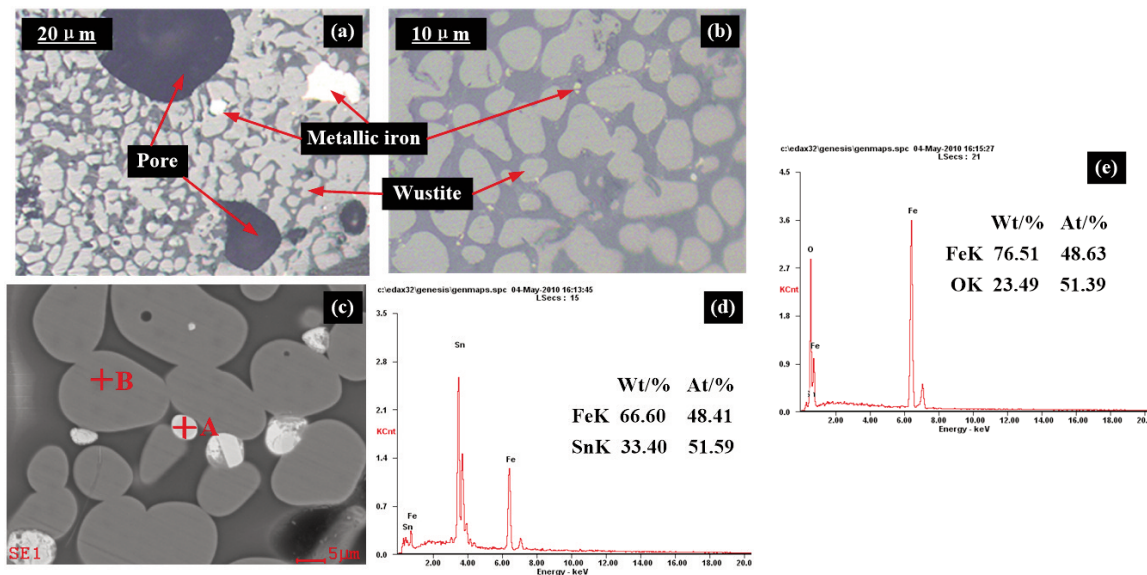


Figure 5. Optical and SEM images of the sinter (Sample 5[#]) ((a) and (b) optical micrograph, (c) SEM micrograph, (d) EDS of spot A, (e) EDS of spot B.)



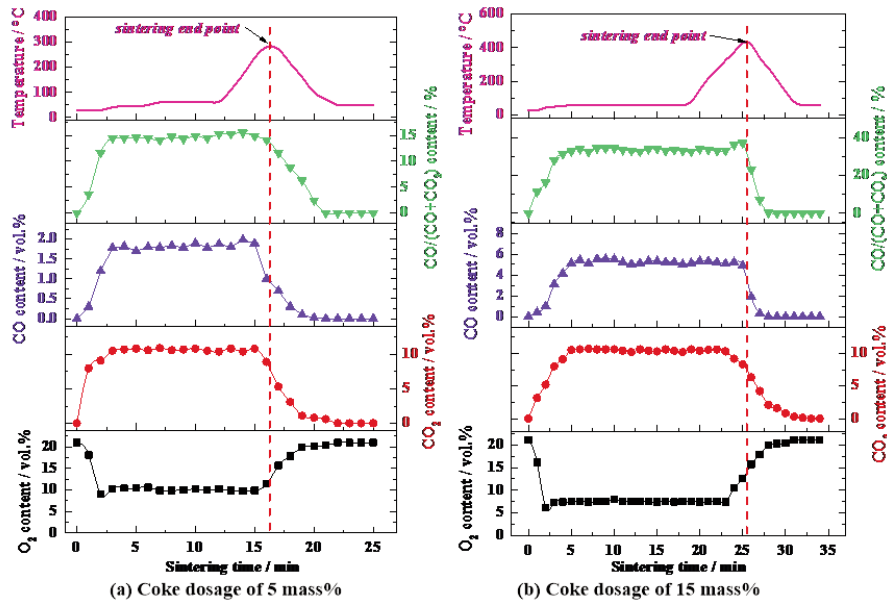


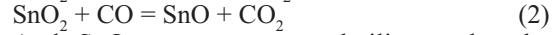
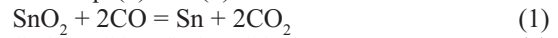
Figure 6. Emission rules of O_2 , CO , CO_2 , $CO/(CO+CO_2)$ contents and temperature of the outlet flue gas (Tested at sample point A in Fig. 2)

sintering temperature and $CO/(CO+CO_2)$ content.

As shown in Fig. 8, previous researches indicated that Fe_2O_3 and SnO_2 were synchronously reduced stepwise according to $Fe_2O_3 \rightarrow Fe_3O_4 \rightarrow FeO \rightarrow Fe$ and $SnO_2 \rightarrow SnO \rightarrow Sn$ [9, 13, 14].

Combined with the previous researches, the main reactions of SnO_2 during the RSP are summarized and

listed as Eqs.(1) and (2).



And SnO was easy to volatilize under the temperature higher than $900^\circ C$. Therefore, in order to remove tin from the tin-bearing iron concentrates by a selective reduction method, the process should be controlled under conditions of FeO (or Fe_3O_4) and $SnO_{(g)}$ (Eq.(1)) being steady existence at a higher temperature (shadow region in Fig. 8).

The reduction of iron oxides and tin oxides start when the temperature is higher than about $500^\circ C$, it means that reduction and volatilization reactions only happen in Stage I (in Table 6 and Fig. 7) of the sintering process. Previous researches proved that the

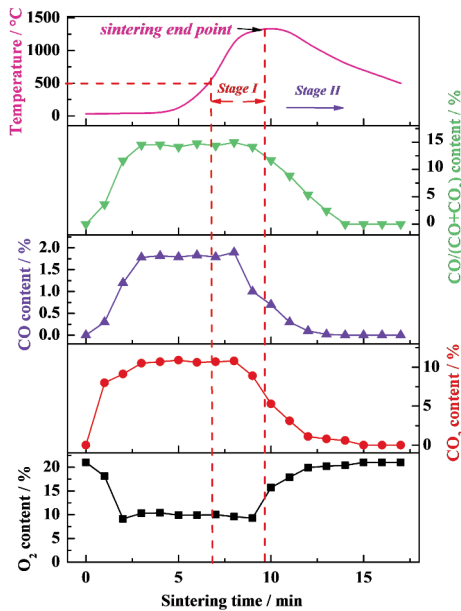


Figure 7. Changing rules of O_2 , CO and CO_2 content of the flue gas and temperature in the sinter bed (Coke dosage of 5.0 mass%, tested at sample point B in Fig. 2)

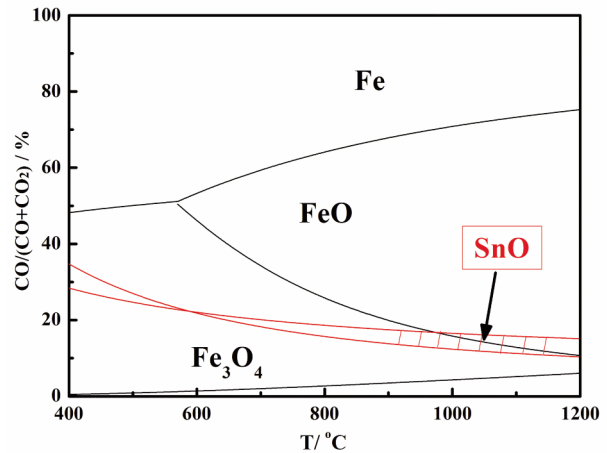


Figure 8. Gas-phase equilibrium diagram of SnO_x and FeO_x in $CO-CO_2$ atmospheres [9, 13, 14]



Table 6. Changing rules of gas components and temperature during the RSP

Stages	CO/(CO+CO ₂)	Temperature
Stage I (before approximating the sintering end-point)	Stabilizing at 15-35 vol.% with coke dosage of 5-15 mass%	Increasing from about 500 °C to 1100 °C
Stage II (approximating the sintering end-point)	Decreasing to zero sharply	Increasing to the top-sintering temperature (> 1300°C) and then decreasing

content of CO/(CO+CO₂) should be controlled at about 20-50 vol.% at the temperature varying from 950°C to 1100 °C in order to remove tin from tin-bearing iron concentrates [9, 13, 14]. Based on above analysis, it can be concluded that the CO/(CO+CO₂) value during the RSP (in Stage I) is theoretically suitable for the volatilization of SnO. However, the short high-temperature residence time and exorbitant sintering temperature (higher than 1100 °C) had adverse effect on the removal of tin, which would result in the over reduction of SnO₂ to metallic tin as Eq.(2).

In summary, the fluctuating sintering atmosphere, temperature and short high-temperature residence time in the RSP is unsuitable for the volatilization of SnO. In order to utilize the tin-bearing iron concentrates in a large scale as the sintering material, the Sn content in the blending materials should be strictly controlled.

4. Conclusions

1) The predominant mineral constituents of the finished sinters were found as wustite and magnetite under the optimal parameters for the RSP. About 30 mass% of tin can be deprived as the form of SnO_(g) from the tin-bearing iron concentrates by the RSP. And the residual tin-bearing phases in the finished sinters were stannic (Sn⁴⁺), stannous (Sn²⁺) compounds and metallic Sn (Sn⁰).

2) The CO/(CO+CO₂) value of the flue gas during the RSP is theoretically suitable for the volatilization of SnO, but the short high-temperature residence time and exorbitant sintering temperature (high than 1100 °C) had an adverse effect on the removal of tin.

3) It seems that the RSP is an available process to utilize these tin-bearing iron concentrates. However, low Sn-containing iron concentrates was need to dilute the Sn content of sinter mix, which should be controlled below 0.12 mass% in order to produce qualified sinters for BF iron-making.

Acknowledgments

The authors would express their heartfelt thanks to National Natural Science Foundation of China (No. 51574283), the Natural Science Foundation of Hunan Province, China (No. 2016JJ2143), Co-Innovation Center for Clean and Efficient Utilization of Strategic Metal Mineral Resources, and Hunan Provincial Innovation Foundation for Postgraduate (CX2015B054).

References

- [1] P.L. Li, Y. Xie, Conserv. Util. Miner. Resour., 4 (2003) 13-16. (in Chinese)
- [2] C.J. Xie, Hunan Nonferrous Met., 11 (1996) 13-17. (in Chinese)
- [3] T. Jiang, Y.B. Zhang, Z.C. Huang, G.H. Li, Trans. Nonferrous Met. Soc. China, 15 (2005), 902-907.
- [4] Y.B. Zhang, L.Y. Chen, G.H. Li, T. Jiang, Z.C. Huang, J. Cent. South Univ. (Science and Technology), 42 (2011) 1501-1508, (in Chinese).
- [5] Y.B. Zhang, T. Jiang, G.H. Li, Z.C. Huang, Y.F. Guo, Ironmaking and Steelmaking, 38 (2011), 613-619.
- [6] Y.B. Zhang, G.H. Li, T. Jiang, Y.F. Guo, Z.C. Huang, Int. J. Miner. Process., 110-111 (2012), 109-116.
- [7] Y.B. Zhang, B.B. Liu, Z.J. Su, J. Chen, G.H. Li, T. Jiang, J. Min. Metall. Sect. B-Metall. 52 (1) B (2016) 9-15.
- [8] Y.B. Zhang, Z.J. Su, B.B. LIU, Y.L. Zhou, T. Jiang, G. H. Li, Powder Technology, 291 (2016), 337-343.
- [9] Y.B. Zhang, B.B. LIU, Z.J. Su, J. Chen, G. H. Li, T. Jiang, Int. J. Miner. Process., 144 (2015), 33-39.
- [10] Z.J. Su, Y.B. Zhang, B.B. LIU, Y.L. Zhou, T. Jiang, G. H. Li, Powder Technology, 292(2016), 251-259.
- [11] Z.J. Su, Y.B. Zhang, B.B. LIU, J. Chen, G. H. Li, T. Jiang, Mineral Processing and Extractive Metallurgy Review, 37 (2016), 179-186.
- [12] W.S. Huang, Stannum, Metallurgical Industry Publishing Company, Beijing, 2001. (in Chinese)
- [13] G.H. Li, Z.X. You, Y.B. Zhang, M.J. Rao, P.D. Wen, T. Jiang, JOM, 66 (2014), 1701-1710.
- [14] Y.B. Zhang: PhD thesis Central South University, Changsha, 2006. (in Chinese)
- [15] T.J. Chun, D.Q. Zhu, Metallurgical and Materials Transactions B, 46 (2014) 1-4.
- [16] S. Machida, H. Sato, K. Takeda, JFE technical report, 5 (2009) 7-13.
- [17] D.Q. Zhu, J. Pan, A.P. He, J. Li, X.F. Xu, Z.Y. Wang, J. Cent. South Univ. (Science and Technology), 36 (2005), 944-948. (in Chinese)
- [18] H.L. Zhang, M.J. Rao, Z.Y. Fan, Y.B. Zhang, G.H. Li, T. Jiang, ISIJ Int., 52 (2012) 2139-2144.
- [19] GB/T 6730.5-2007: AQSIQ and SAC, (2007). (in Chinese)
- [20] GB/T 6730.6-1986: AQSIQ and SAC, (2007). (in Chinese)
- [21] GB/T 6730.8-1986: AQSIQ and SAC, (2007). (in Chinese)
- [22] GB/T 1819.2-2004: AQSIQ and SAC, (2004). (in Chinese)
- [23] Y. Zhao, H. X. Ruan, Metallurgical analysis, 20 (2000), 29-31. (in Chinese)

